On the Critical Flow of Vapor Liquid Mixtures by Cruver and Moulton

D. L. LINNING and M. A. H. G. ALDERSON

United Kingdom Atomic Energy Authority, Risley, England

We have recently observed that the critical flow chart for two-phase expansion of water provided in the above cited (*1*) paper gives predictions which are very close to those made by the present writers in their paper (*2*) published earlier this year. A comparison of predicted values is given below, for an outlet quality $X = 10\%$.

Outlet Pressure (lb./sq.in.abs.)	500	200	100	50	25	10
Critical Mass Flow (lb./sq.ft. sec.)						
Cruver and Moulton Predictions	6,200	3,200	1,900	1,100	550	270
Linning, Pexton, Alderson Predictions	6,500	3,400	1,900	1,100	600	270

These results show a remarkable similarity and, at first sight, seemed to lend mutual support for two theories which have little else in common.

The Cruver and Moulton theory is based on the postulate that at the critical outlet condition the phase velocity ratio is the cube root of the phase specific volume ratios (corresponding to minimum kinetic energy for a given mass flow or maximum mass flow for a given kinetic energy). The other theory is derived using the three basic conservation laws to arrive at six equations of flow. These can be integrated numerically in a step-by-step process which follows the expansion until critical outlet conditions are reached. Beyond this point the equations are incompatible. The critical outlet condition can also be recognized by the approach of the ratio $-VdP/d(KE)$ to unity, where V is the specific volume, P the pressure, and (KE) the kinetic energy of steam-water mixture, that is $-VdP$ is the maximum rate of conversion of internal to kinetic energy which is theoretically possible. Empirical information in the shape of wall and interphase friction factors is required to obtain a numerical solution to the two-phase flow equations. It might be considered on the evidence of the above comparison that the two theories lend some support to each other, but further examination reveals that this is not so. The Cruver-Moulton theory leads to a critical outlet velocity ratio of 9.8 whereas the other theory predicts a corresponding value of 15.3. Furthermore, it is found that in this particular case the fluid kinetic energy is practically unchanged over the velocity ratio range 8 to about 20 as shown in the graph. It follows, rather surprisingly, that an arithmetically correct prediction of critical mass flow for specified outlet pressure and quality is not a sensitive test of the validity of any theory.

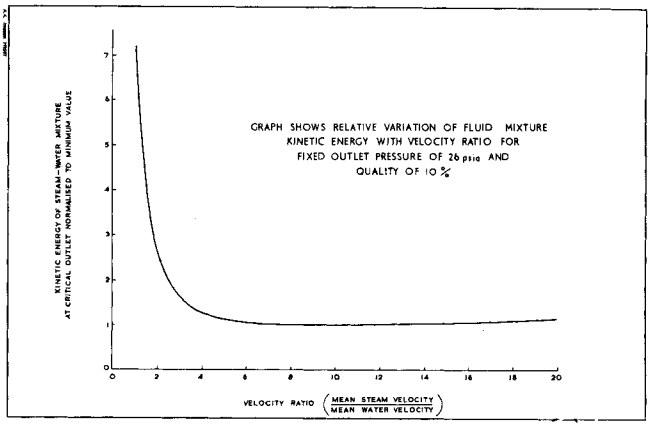

Fig. 1. Variation of fluid mixture kinetic energy.

Perhaps it should be added that we are discussing here the situation which would prevail if thermodynamic equilibrium conditions were to obtain throughout an expansion and that while this is of considerable theoretical interest, in practice deviations from thermodynamic equilibrium near the critical outlet significantly affect actual flow behavior.

LITERATURE CITED

1. Cruver, J. E., and R. W. Moulton, *AIChE J.*, 13, 52 (1967).
2. Linning, D. L., A. F. Pexton, and M. A. H. G. Alderson, *J. Mech. Eng. Sci.*, 10, No. 1, 64 (Feb., 1968).

Diffusion in Membrane-Limited Blood Oxygenators

M. H. WEISSMAN

Carnegie-Mellon University, Pittsburgh, Pennsylvania

Membrane blood oxygenators mimic natural lungs in separating blood and gas phases by a permeable membrane. Resistance to gas transfer is contributed by both membrane and blood film, but the ultimate limit on the

efficiency of a membrane oxygenator is imposed by the properties of the membrane. To reach this ultimate limit, when diffusion is limited only by the membrane, it is necessary to reduce the diffusional resistance of the blood film to an insignificant level. This may be done through introduction of convection or by use of a very thin blood film (*1* to *3*). In this work it is assumed that suitable convection is present; the mechanism for generating such convection will be the subject of a later paper.

In a membrane limiting situation, gas transfer rates may be predicted by solving a linear diffusion equation for oxygen in the membrane, together with a nonlinear boundary condition, at the blood-membrane interface, imposed by the oxygen absorption characteristics of the blood. [Gases obey Henry's law in most polymeric membranes and penetrate them by diffusion rather than by passage through membrane pores (*4*)].

THE PROBLEM

With reference to Figure 1, the well-mixed blood in the channel at any axial distance, z, has a local oxygen content which is independent of x and y. Thus, neglecting axial diffusion, the diffusion equation is simply:

$$D_{O_2,m}\frac{\partial^2 P_{O_2}(y,z)}{\partial y^2} = \overline{w}\frac{\partial P_{O_2}(y,z)}{\partial z}, \quad \begin{matrix} 0 \leq y \leq t \\ 0 \leq z \end{matrix} \qquad (1)$$

where $D_{O_2,m}$ is the diffusivity of oxygen in the membrane, P_{O_2} is the oxygen concentration in the membrane divided by the solubility of gas in membrane or the membrane partial oxygen pressure, t is the membrane thickness and $\overline{w}$ is the average blood velocity or blood discharge rate divided by the channel cross-sectional area, L^2/N. This steady problem is equivalent to unsteady diffusion in a rod of length t, with a time variable equal to $z/\overline{w}$.

If Equation (1) were multiplied throughout by the solubility of oxygen in the membrane, $S_{O_2,m}$, a more conventional equation, in terms of oxygen concentration would appear. The formulation in terms of partial pressures is convenient as oxygen concentration is discontinuous across a blood-membrane interface, whereas partial pressure is not.

The initial and boundary conditions for Equation (1) are:

$$P_{O_2}(t,z) = (P_{O_2})_\infty, z \geq 0$$

$$P_{O_2}(0,0) = (P_{O_2})_0$$

The first condition relates to the membrane-gas interface and states that the atmospheric partial pressure is $(P_{O_2})_\infty$ for all z. The second condition states that at the channel inlet the partial pressure in the blood plasma is $(P_{O_2})_0$. At the membrane-blood interface ($y = 0$) the partial pressure on the membrane surface is equal to that in the plasma, since P_{O_2} is continuous across the interface. As oxygen enters the moving blood, its plasma partial pressure rises in a nonlinear fashion, controlled by the oxy-hemoglobin dissociation curve. This curve relates total O_2 content of blood to plasma P_{O_2} (see Figure 2). Total oxygen content is generally given in a normalized form termed saturation. A saturation, S_{O_2}, of 100% means that (nominally) 9.1×10^{-3} moles of O_2 are present, in all forms, per liter of blood. At any axial distance downstream the blood oxygen content increase is the integral of the product of O_2 flux through the membrane times membrane area, divided by the blood flow rate. The saturation increase is just $100/T_{O_2}$ times this (where $T_{O_2} = 9.1 \times 10^{-3}$ moles/liter). Thus at $z = z_1$, the saturation increase is:

$$\Delta S_{O_2}(z_1) = \frac{100}{T_{O_2}}\left[\frac{D_{O_2,m}S_{O_2,m}}{\overline{w}L^2/N}\int_0^{z_1}\left.\frac{\partial P_{O_2}}{\partial y}\right|_{y=0} Ldz\right] \qquad (2)$$

where the constant diffusivity and solubility have been taken out of the integral.

If the oxy-hemoglobin dissociation curve is $S_{O_2} = g(P_{O_2})$, then the boundary condition at $y = 0$, for $z > 0$, is that the partial pressure is the value at $z = 0$, plus the increase:

$$P_{O_2}(0,z) = g^{-1}[(S_{O_2})_0 + \Delta S_{O_2}(z)] \qquad (3)$$

where g^{-1} is the inverse function of g and $(S_{O_2})_0 = g[(P_{O_2})_0]$.

A convenient dimensionless form results from letting

$$y^* = y/t, \quad z^* = \frac{zD_{O_2,m}}{t^2 w}$$

The dimensionless equation and boundary conditions resulting are

$$\frac{\partial^2 P_{O_2}}{\partial y^{*2}} = \frac{\partial P_{O_2}}{\partial z^*}, \begin{matrix} 0 \leq Y^* \leq 1 \\ 0 \leq z \end{matrix} \qquad (4)$$

and

$$P_{O_2}(y^*,0) = (P_{O_2})_0$$

$$P_{O_2}(1,z^*) = (P_{O_2})_\infty$$

$$P_{O_2}(0,z^*) = g^{-1}\left[(S_{O_2})_0 + \frac{100N(S_{O_2,m})t}{T_{O_2}L}\int_0^{z^*}\left.\frac{\partial P_{O_2}}{\partial y^*}\right|_{y^*=0} dz^*\right] \qquad (5)$$

Little profit accrues from nondimensionalizing P_{O_2}, as g and g^{-1} are not linear.

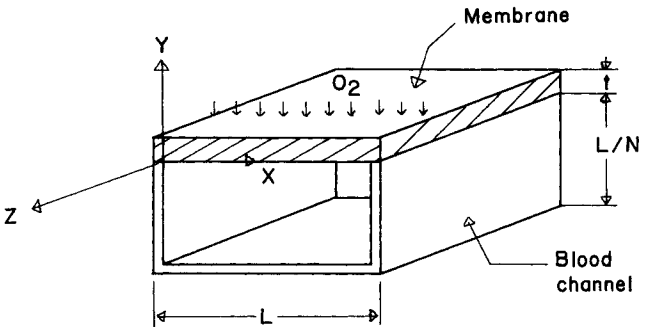

Fig. 1. Cross section of blood flow channel. Blood is continuously mixed to destroy diffusional resistance (generation of mixing not shown here) and flows with average velocity $\overline{w}$ in the z direction.

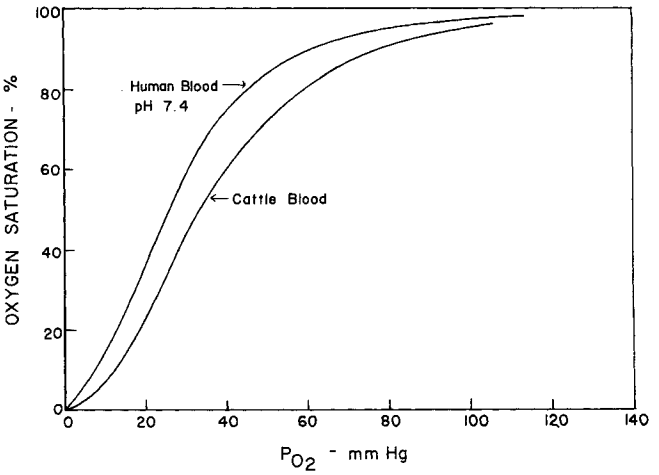

Fig. 2. Oxygen saturation vs. P_{O_2}. (Oxygen saturation is the total oxygen carried by plasma and red cells; 100% represents a total oxygen content of 9.1×10^{-3} moles/liter.)

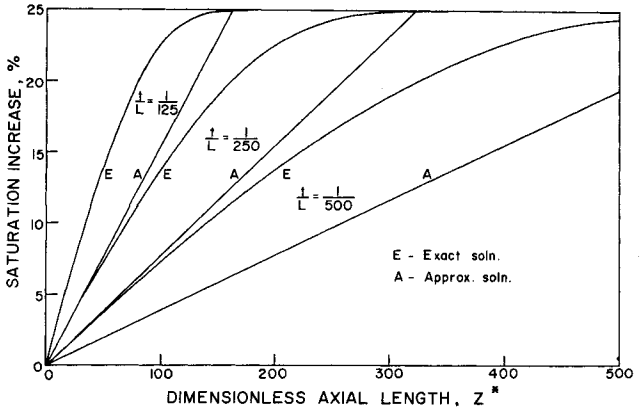

Fig. 3. Saturation increase vs. z^*, exact and approximate solutions. $(P_{O_2})_\infty$ is 150 mm. Hg. and the aspect ratio is 2.

NUMERICAL SOLUTION

The solubility $S_{O_2,m}$, the ratio (t/L), N and T_{O_2} must be specified to effect a solution of Equations (4) and (5). Currently, a dimethyl silicone rubber membrane offers least resistance to gas transfer of all known membranes. The oxygen solubility for this membrane is 1.82×10^{-5} moles/liter-mm. Hg. (4). The maximum oxygen content for average whole blood is 9.1×10^{-3} moles/liter. Equation (4) was solved numerically assuming (t/L) ratios of 1/125, 1/250 and 1/500. The values 150, 300, and 750 mm. Hg. were taken for $(P_{O_2})_\infty$, and 54 mm. Hg. for $(P_{O_2})_0$, that is the venous saturation was 75%. The channel aspect ratio, N, was taken as 2 and the function g was fitted by the difference of a constant and two decaying exponentials (1). It is convenient to use exponentials for the fit, as the oxy-hemoglobin dissociation curve saturates at high values of P_{O_2}. Past experience has shown that solutions are not sensitive to small changes in the fitting of g. In fact, solutions for human and cattle blood are nearly indistinguishable (1).

The equation was solved using an explicit, finite difference method with 20 equal increments in y^*. The ratio of z^* to y^* spacing was given by $\Delta z^*/(\Delta y^*)^2 = 0.25$. Accuracy of the solution was verified by repeating one solution with 40 increments in y^*. No significant differences between the 20 and 40 point solutions were noted and the maximum variation between the two amounted to one part in 2,500.

Figure 3 shows the increase in blood oxygen saturation vs. z^* for various (t/L) ratios. Decreasing the ratio (t/L) shifts the curve to the right, as for a fixed axial hydrostatic pressure gradient the blood flow rate increases as L^2, whereas the membrane area increases as L. For fixed membrane thickness, decreasing (t/L) reduces the ratio of membrane area to blood flow rate, necessitating increased axial length in order to attain a given saturation increase.

Also shown in Figure 3 are approximate solutions which assume that a constant pressure gradient, $[(P_{O_2})_\infty - (P_{O_2})_0]/2$, acts across the membrane all along its length. For this case

$$S_{O_2}(z^*) = (S_{O_2})_0 + \frac{100(S_{O_2,m})t}{T_{O_2}L}[(P_{O_2})_\infty - (P_{O_2})_0]z^* \qquad (6)$$

Figure 3 demonstrates that use of an average pressure gradient provides a fair approximation to the channel length required for complete oxygen equilibration of gas and blood. For saturation increases less than that corresponding to equilibration, the approximate solutions are always conservative, predicting channel lengths up to 100% too large for the required oxygen transfer.

Nondependence of Solution on Nt/L

If the curves of Figure 3 are plotted against Ntz^*/L they appear, very nearly, to be colinear. This behavior cannot be predicted *a priori* from the dimensionless equation and boundary condition, as Nt/L would appear from them to be a system parameter. The explanation of this paradox is due, in part, to the tendency of the red cells, acting as oxygen sinks to retard rapid axial changes in oxygen tension at the blood membrane interface. Thus the diffusion in the membrane reaches a pseudo steady state in which:

$$\frac{\partial P_{O_2}(y^*,z^*)}{\partial y^*} \approx (P_{O_2})_\infty - P_{O_2}(z^*) \Big|_{y^*=0}$$

This approximation was confirmed by the results of the numerical analysis. Figure 4 shows that curves of P_{O_2} vs. y^* are nearly linear over a wide range of values of z^*, for the case $(t/L) = 1/125$.

Noting that the saturation increase at any axial distance can be obtained from Equation (6), we examine the relationship between the axial lengths, z_1^* and z_2^*, required to achieve identical saturation increases in two separate channels with $N(t/L)$ ratios of $N_1(t/L)_1$ and $N_2(t/L)_2$, respectively. Since the saturation increases are the same in both channels we note

$$N_1\left(\frac{t}{L}\right)_1 \int_0^{z_1^*} \frac{\partial P_{O_2}}{\partial y^*}(z^*) \Big|_{\substack{y^*=0 \\ (Nt/L)_1}} dz^* = N_2\left(\frac{t}{L}\right)_2 \int_0^{z_2^*} \frac{\partial P_{O_2}}{\partial y^*}(z^*) \Big|_{\substack{y^*=0 \\ (Nt/L)_1}} dz^* \qquad (7)$$

By a change of variables $x = z^*/z_1^*$:

$$\int_0^{z^*_1} \frac{\partial P_{O_2}}{\partial y^*}(z^*) \Big|_{\substack{y^*=0 \\ (Nt/L)_1}} dz^* = z_1^* \int_0^1 \frac{\partial P_{O_2}}{\partial y^*}(xz_1^*) \Big|_{\substack{y^*=0 \\ (Nt/L)_1}} dx \qquad (8)$$

and therefore applying Equation (8) to the left-hand side of Equation (7) and a similar form to right-hand side:

$$N_1\left(\frac{t}{L}\right)_1 z_1^* \int_0^1 \frac{\partial P_{O_2}}{\partial y^*}(xz_1^*) \Big|_{\substack{y^*=0 \\ (Nt/L)_1}} dx = N_2\left(\frac{t}{L}\right)_2 z_2^* \int_0^1 \frac{\partial P_{O_2}}{\partial y^*}(xz_2^*) \Big|_{\substack{y^*=0 \\ (Nt/L)_1}} dx \qquad (9)$$

Recalling the approximation

$$\frac{\partial P_{O_2}}{\partial y^*} \approx (P_{O_2})_\infty - P_{O_2}(z^*) \Big|_{y^*=0} \approx \frac{\partial P_{O_2}}{\partial y^*} \Big|_{y^*=0}$$

and using this in Equation (9) we note after rearranging:

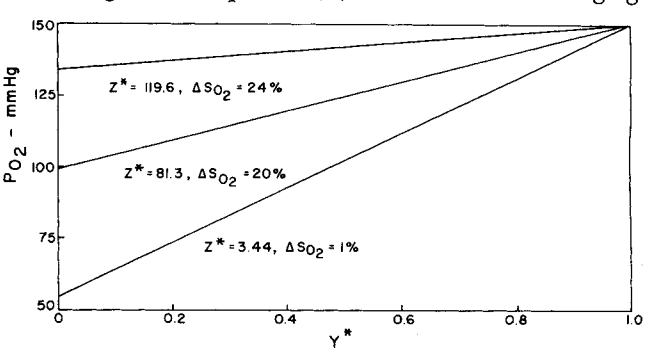

Fig. 4. P_{O_2} vs. y^*, for $N(t/L) = 1/62.5$ and several values of z^*.

$$\frac{N_1\left(\frac{t}{L}\right)_1 \; z_1^*}{N_2\left(\frac{t}{L}\right)_2 \; z_2^*} \approx \frac{\int_0^1 [(P_{O_2})_\infty - P_{O_2}(xz_2^*)\Big|_{\substack{y^*=0 \\ (Nt/L)_2}}]dx}{\int_0^1 [(P_{O_2})_\infty - P_{O_2}(xz_1^*)\Big|_{\substack{y^*=0 \\ (Nt/L)_1}}]dx} \quad (10)$$

The values of the bracketed quantities are identical in both integrals for $x = 0$ and also for $x = 1$. Due to the basic similarity of the two diffusion processes, it is reasonable to expect that the bracketed functions will be nearly identical for all values of x between 0 and 1 as well. Thus, the ratio of the integrals is nearly unity and

$$N_1\left(\frac{t}{L}\right)_1 \; z_1^* \approx N_2\left(\frac{t}{L}\right)_2 \; z_2^* \quad (11)$$

The data used to plot Figure 3 indicate that this approximation is accurate to 1/3 of 1%. For practical purposes the parametric dependence of the solution on the group $N\,(t/L)$ may be dropped.

Figure 5 incorporates this simplification in a plot of saturation increase vs. $N\,(t/L)\,z^*$ for three values of atmospheric oxygen tension: 150, 300, and 750 mm. Hg. The value of 750 mm. Hg corresponds to a nearly pure oxygen atmosphere. The value 300 is chosen so that, considering the average pressure gradient normally available for carbon dioxide removal (about 45 mm. Hg.) and the relative permeabilities of silicone rubber to oxygen and carbon dioxide (about 1 to 5, respectively), the ratio of carbon dioxide removed to oxygen added will be about 0.85, a normal value (*4, 5*). For atmospheric oxygen tensions above 300, the oxygenator design will be limited by the membrane area needed for carbon dioxide removal, for tensions below 300 by the area needed for oxygen addition. Although oxygen transfer may be speeded by increasing $(P_{O_2})_\infty$, as Figure 5 indicates, the carbon dioxide gradient reaches a maximum of 45 to 50 mm. Hg. when $(P_{CO_2})_\infty$ equals zero.

Design Formulae

It is easily shown that the total membrane area and blood priming volume for an M channel oxygenator are

$$\text{Area} = MzL = \frac{Qt}{D_{O_2,m}}\left[N\left(\frac{t}{L}\right) z^*\right]$$

$$\text{Priming Volume} = \frac{MzL^2}{N} = \frac{Qt}{D_{O_2,m}}\left(\frac{L}{N}\right)\left[N\left(\frac{t}{L}\right) z^*\right]$$

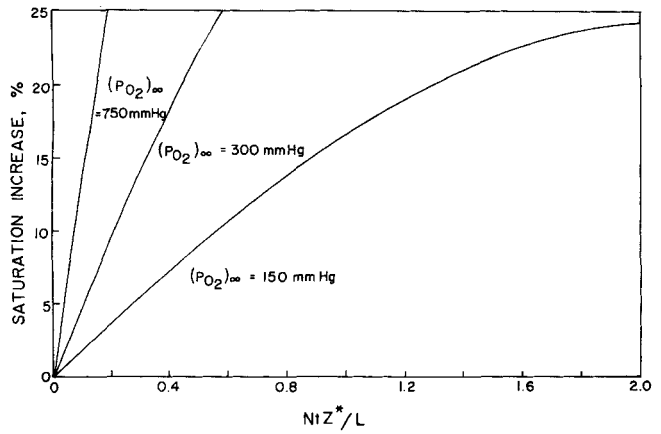

Fig. 5. Saturation increase vs. $N(t/L)z^*$ for three values of $(P_{O_2})_\infty$.

where Q is the total blood flow rate.

For given values of $(P_{O_2})_\infty$ and the desired saturation increase, the square bracketed term is constant. Therefore the priming volume may be made as small as desired by choosing an appropriately small L. [Considerations relating to the generation of convection in the blood set a lower limit on L, however (*6*).] The membrane area is fixed by the membrane material, blood flow rate and oxygen boundary conditions. It is independent of channel geometry.

CONCLUSION

The numerical method illustrated here is of use in predicting gas transfer characteristics of membrane-limited, optimally designed oxygenators. The solutions were found to depend on the boundary conditions and the blood and membrane physical properties, but not on the channel aspect ratio or the ratio of membrane thickness to channel width. The method may be applied, with minor modifications to situations involving other membrane materials, other nonrectangular blood channel geometries and other reacting blood gases. It is applicable, with small changes, to situations involving nonbiological reacting fluids, as well. An approximate method, using an average pressure gradient, was seen to be a good predictor of the channel length at which equilibration is nearly completed.

For a given saturation increase and given boundary and initial values of P_{O_2}, the membrane area of an optimally designed oxygenator is independent of channel size, geometry, and the number of channels used. Under the same conditions the priming volume decreases linearly with channel width.

ACKNOWLEDGMENT

The author would like to thank the Carnegie-Mellon University Computation Center for their generous donation of the computer time used in the preparation of this paper. He would also like to acknowledge the support of NIH grant No. HE 12714.

NOTATION

$D_{O_2,m}$ = diffusivity of oxygen in membrane
g = a function relating oxygen saturation to plasma partial oxygen pressure
g^{-1} = inverse of g
L = channel width
N = ratio of channel width to depth
P_{O_2} = partial pressure of oxygen
S_{O_2} = oxygen saturation
$S_{O_2,m}$ = solubility of oxygen in membrane
t = membrane thickness
T_{O_2} = oxygen content of saturated blood, 9.1×10^{-3} moles/liter
$\bar{w}$ = average axial velocity of blood
x, y, z = rectangular coordinates
y^*, z^* = dimensionless coordinates
$(\,)_\infty$ = condition at $y = t$
$(\,)_0$ = condition at $z = 0$

LITERATURE CITED

1. Weissman, M. H., and L. F. Mockros, *J. Eng. Mech. Div., EM 6*, 93, 225 (1967).
2. *Ibid., EM* 3, 94, 857 (1968).
3. Weissman, M. H., and T. K. Hung, *Proc. 21st Ann. Conf. Eng. Medicine Biol.*, Houston, Tex., (Nov. 1968).
4. Robb, W. L., *Rept. No. 65-C-031*, Genl. Elec. Co. (Oct. 1965).
5. Ruch, T. C., and J. F Fulton, "Medical Physiology and Biophysics," W. B. Saunders, Philadelphia, Pa. (1955).
6. Weissman, M. H., and T. K. Hung, *AIChE J.*, to be published.